

Detecting negative ions onboard small satellites

Enter authors here: S. T. Lepri¹, J. M. Raines¹, J. A. Gilbert¹, J. Cutler², M. Panning³, and T. H. Zurbuchen^{1,2}

¹ The University of Michigan, Department of Climate and Space Sciences and Engineering, ² The University of Michigan, Department of Aerospace Engineering, ³Orbital ATK,

Corresponding author: Susan T. Lepri (slepri@umich.edu)

†Additional author notes should be indicated with symbols (for example, for current addresses).

Key Points:

- Surface interactions with dust grains in the heliosphere and near the moon can produce negative ions
- The contribution of negative ions to the heliosphere and lunar environment are largely unknown
- AIPS is a small compact, yet capable anion sensor for use on small satellites.

This is the author manuscript accepted for publication and has undergone full peer review but has not been through the copyediting, typesetting, pagination and proofreading process, which may lead to differences between this version and the [Version of Record](#). Please cite this article as doi: [10.1002/2016JA023327](https://doi.org/10.1002/2016JA023327)

Abstract

Recent measurements near comets, planets, and their satellites have shown that heavy ions, energetic neutral atoms, molecular ions and charged dust contain a wealth of information about the origin, evolution, and interaction of celestial bodies with their space environment. Using highly sensitive plasma instruments, positively charged heavy ions have been used to trace exospheric and surface composition of comets, planets and satellites as well as the composition of interplanetary and interstellar dust. While positive ions dominate throughout the heliosphere, negative ions are also produced from surface interactions. In fact, laboratory experiments have shown that oxygen released from rocky surfaces is mostly negatively charged. Negative ions and negatively charged nanograins have been detected with plasma electron analyzers in several different environments (e.g., by Cassini and Rosetta), though more extensive studies have been challenging without instrumentation dedicated to negative ions. We discuss an adaptation of the Fast Imaging Plasma Spectrometer (FIPS) flown on MESSENGER for the measurement of negatively charged particles. MESSENGER/FIPS successfully measured the plasma environment of Mercury from 2011 until 2015, when the mission ended, and has been used to map multiple ion species (H^+ through Na^+ and beyond) throughout Mercury's space environment. Modifications to the existing instrument design fits within a 3U CubeSat volume, and would provide a low mass, low power instrument, ideal for future CubeSat or distributed sensor missions seeking, for the first time, to characterize the contribution of negative particles in the heliospheric plasmas near the planets, moons, comets and other sources.

1 Introduction

Positive ions have been ubiquitously observed throughout the Universe, and in particular have been directly observed throughout the heliosphere and around planetary atmospheres [e.g. Larsson et al. 2012 and references therein]. Because of the tenuous nature of planetary and interplanetary environments, ionized material can persist in such a state. The resulting plasma environments are formed through a number of ongoing processes that provide both sources and sinks for charged material. The largest source of ions in the heliosphere is the Sun, which accelerates highly charged particles into the heliosphere via the solar wind (e.g. H^+ , He^{2+} , C^{5+} , O^{6+} , Fe^{10+}). Additional local sources of ions include interstellar dust, interplanetary dust and sputtered particles from planetary, cometary or satellite surfaces, which have been ionized by solar UV radiation, electron ionization, or via charge exchange with solar wind particles. Additionally exospheric escape for charged particles can occur at a variety of planets. Many of the ions from local sources are singly positively charged, but other ionic charge states exist.

While much is known about the sources and behavior of positive ions in the heliosphere, until recently, little was known about the sources and behavior of negative ions. The search for negative ions in the heliosphere begins with the search for much of the same dust and neutral material that produces the positive ions described above. There are a variety of sources of dust in the heliosphere (e.g. including the "inner source"), some left behind by comets, some resulting

from asteroid collisions, some ejected the surfaces and atmospheres of planets and their satellites, and some from the interstellar medium, through which the heliosphere is moving [Gloeckler et al. 2000; Klahr and Lin, 2001; Frisch et al. 1999].

Negative ions can be produced via a number of processes, including through gas-phase chemistry, by interaction with solar photons via photon-stimulated desorption (PSD), electron stimulated desorption (ESD), charge exchange between ions and neutrals or dust, or solar wind plasma sputtering on planetary regolith and interstellar and interplanetary dust grains [Domingue et al., 2014 and references therein]. Negative ion production on the surfaces of the Moon and from heliospheric dust grains have been predicted, but they have yet to be observed even though they may constitute a significant component of material at the Moon and in the heliosphere, and a powerful indicator of the physical processes that govern plasma interactions and space weathering. Negative ions have been observed in Earth's ionosphere, as well as in the ionospheres of satellites of Jupiter and Saturn [Larsson et al., 2012; Coates et al., 2007; Coates et al 2007, 2009, 2010a and b; Wekhof, 1981, and references therein]. They have also been observed in Mars atmosphere and near comets [e.g., Halekas et al. 2015, Burch et al 2015, Coates et al., 2007, Hargreaves 1992, Chaizy et al., 1991, Borucki et al., 2006]. Coates et al. [2007] reported the discovery of negative ions in Titan's atmosphere up to an altitude of ~950 km using data from the Electron Spectrometer (ELS) as part of the Cassini Plasma Spectrometer (CAPS). These negative ions were observed as a very narrow, cold contribution to the electron spectra and were observed as Cassini plowed through the plasma with a ram speed of ~6 km/s. Additionally, the observation of negative ions at these altitudes in Titan's atmosphere was surprising, as they were not expected to be present above 100km. Chaizy et al. [1991] reported the first observations of negative ions in cometary material.

Shortly after these findings, Cassini CAPS-ELS and IMS also identified negative ions and negatively charged nanograins in the south polar plume of Enceladus [Coates et al., 2009, Hill et al. 2012]. Negatively charged nanograins with masses of the order 10^2 - 10^5 amu, have also been reported from the Rosetta mission (e.g. Burch et al. 2015, Gombosi et al. 2015). These negatively charged nanograins are seen both coming from the direction of the comet and also coming from the solar direction with energies in the 1-20 keV range. Additionally, both negatively and positively charged nanograins have been observed near Enceladus by the Cassini CAPs sensors (Jones et al. 2009, Hill et al. 2012) as well as near Saturn's moon, Rhea (Teolis et al 2010), and potentially near Dione (Tokar et al (2012)). The existence of the negatively charged nanograins near comets and satellites indicates that the negatively charged particles are present and observable when conditions are right in the space environment. Both the discovery of negative ions and negatively charge dust grains in a variety of space environments motivates the need to further study these populations.

The dominant physical mechanism that accelerates negative ions and nanograins is expected to be the pickup process in the solar wind. While a neutral gas or dust particle may initially have negligible energy (~few eV), once ionized, they are subjected to a Lorentz force

within the interplanetary magnetic field convecting away from the Sun via the solar wind [Vasyliunas and Siscoe, 1976]. Newly picked up ions will gyrate around the magnetic field, with an orbit initially defined by the initial velocity component perpendicular to the magnetic field. The pickup ion velocity distribution evolves, as the particle scatters on magnetic irregularities, from a ring distribution shortly after pickup to a spherical shell distribution until the particles scatter to fill a sphere in velocity space centered on the solar wind speed, with a radius of one solar wind speed [Gloeckler et al., 1997; Gloeckler and Geiss, 1998; Kallenbach 2000 and references therein; Neugebauer et al., 1989, Coates et al., 1989, 1990, 2015, Coates 2012]. This flattened distribution in velocity space is fit with multiple parameters and show as curves in Figure 1, which rolls over around two solar wind speeds. The Gaussian peaked distribution in the middle of the pickup ion distribution is the superposition of the solar wind protons on top of the pickup protons. The characteristic shoulder in the distribution at two solar wind speeds makes pickup ions clearly distinguishable from the bulk solar wind. However, the exact shape of the pickup ion distribution depends on the injection speed of the initial neutral particle before it became charged and picked up in the solar wind electric field (e.g. Coates et al 1989). While solar wind protons, making up 98% of the solar wind, can obfuscate a large portion of velocity space shared with pickup ions with their large flux, the same issue is not present for negative ions. Hence, negative ions should be more easily distinguishable since the background flux should nearly negligible, assuming their lifetime before photo-dissociation is long enough for them to make it into the instrument.

Measurements made to date provide evidence that negatively charge particles exist in neutral gas or dusty environments and motivate further investigation into additional sources of negative ions in the heliosphere. The measurements discussed above were typically performed with instruments optimized for other purposes (e.g. electron analyzers), and have thus been very limited. In these observations, it is not possible to easily determine the composition of these particles nor is it possible to determine whether they are singly charged grains or atomic negative ions.

A mission concept is presented to provide a unique opportunity to survey several different plasma environments on its trajectory out of the Earth's atmosphere, during a flyby of the Moon, and as it settles into a heliocentric orbit. The goal of the concept mission is to measure and map contributions of negative heavy particles in the space environment. The science goals are to examine and analyze negative ions and other negatively charged particles and their sources near the Earth, the Moon, and in other parts of the heliosphere using an optimized Anion Imaging Plasma Spectrometer (AIPS). These measurements will put improved constraints on the abundances of dust and neutrals, surface processes on airless bodies, and on other sources of negative particles in the heliosphere. The proposed mission would provide the measurements of these negative particles with sufficient resolution to characterize a broad range of plasma environments, with high temporal and spatial resolution.

This paper will present this mission concept and expected measurements. Section 2 will describe the science objectives of such an investigation, and section 3 will provide a mission overview to demonstrate that this investigation can indeed be carried by a single 6U CubeSat. We conclude in section 4, that this mission can provide the first dedicated measurements of negative particles that will allow us to characterize the composition of these particles in a range of environments throughout the heliosphere and quantify their contribution to the local pickup ion population.

2. Measurement Objectives

Our dedicated investigation has two complementary science objectives.

Measurement Objective 1: Negative particles in the Heliosphere

This mission objective focuses both on ions and also nanograins from heliospheric sources. Due to the lifetime of negative ions, on the order of seconds, most of the negatively charged particles originating in the heliosphere are expected to be negatively charged nanograins. But, there are also ionic sources such as from extended and localized sources described below.

Dust components: Interplanetary space is filled with gas, plasma, and dust, all of which provide sources for positive and negative ion production in the heliosphere. Most dust originates in the outer heliosphere and is transported into the inner heliosphere via comets, collisions, or as it is slowed by the Poynting Robertson effect (Klahr and Lin, 2000). Beta-meteoroids, or sub-micrometer dust particles (e.g., nanograins) can be propelled out of the inner heliosphere due to radiation pressure and contribute to the dust population [Zook et al., 1975; Zook, 1975]. In addition, interstellar dust enters the heliosphere as it moves through the interstellar medium and is focused by the Sun's gravity in the downstream region. While helium makes the largest contribution at the orbit of Earth, H, C, O, Ne are also carried into the heliosphere by the interstellar wind (Kallenbach et al. 2000 and references therein.) McComas et al. (2004) measured heliospheric pickup ions at distances $>6\text{AU}$, likely of interstellar origin.

Inner source: Measurements from Cassini, Galileo and Ulysses indicated a nearly ubiquitous presence of dust between 1 and 5 AU (Schippers et al. 2015 and references therein). The flux near 1AU is measured to be $\sim 0.1 \text{ cm}^{-2} \text{ s}^{-1}$ and falls off with heliocentric distance indicating a source inside of 1AU, perhaps as close as 0.2 AU (Mann et al. 2007). This source of dust in the inner heliosphere, left over from the formation of the solar system or transported from the outer solar system via the Poynting-Robertson effect. This so called "inner-source" is also source of pickup ions, made almost entirely of C and O, but traces of other elements also exist. With no atmosphere to shield them, these dust grains are under intense photon bombardment due to close proximity to the sun. Intense UV radiation can detach neutrals from the dust grains that are then continually bombarded by solar wind plasma and electrons [Geiss et al. 1995]. Solar

wind adsorption from the inner source neutrals makes up a large component of the pickup ions in this region [Gloeckler et al. 2000].

The surface processes described above are active on the surface of interplanetary dust grains and desorbed neutrals and likely provide a pathway for the creation of pickup negative ions as well as neutrals. As dust grains are composed of a large fraction of silicate minerals, similar to all rocky bodies in our solar system they likely undergo similar sputtering processes. Small grains can become negatively charged by plasma electron impact [Hill et al., 2012], which causes an increase in produced of negative secondary ions [Lanzillotto et al., 1991; Larsson et al 2012].

Locally produced negative ions: There is strong evidence for a ubiquitous presence of pickup O^+ carried along with the solar wind, which has been measured in-situ out to 5AU (Geiss et al. 1994). Since, O^- is more likely to form than O^+ (Funsten et al. 1992) in sputtering interactions, the presence of O^+ indicates that it is likely that AIPS will be able to measure O^- , which is locally produced by the solar wind interaction with dust. While the lifetime of O^- may be short at smaller heliocentric radii due to photo-detachment, if the process is ongoing at all heliocentric distances, the sensor is likely to sample O^- , especially at larger heliocentric distances where solar UV has reduced intensity.

Cometary particles: Comets also provide a source of pickup ions in the heliosphere. Comets consist of ice, dust and rocky particles within a nucleus that ranges in sizes up to ~1km in diameter, at smaller heliocentric distances. As cometary ice evaporates, it can release trapped negative ions or it can expel neutrals that can become ionized or molecular clusters with high electron affinity [Burch et al. 2015, Larsson et al. 2012, Jackson 1992, Wekhof. 1981]. Early measurements from Giotto resolved bi-spherical cometary water group ion distributions at comet Halley (Coates et al., 1990). Since then, positive and negative pickup ions have been observed from comets in a number of cases [e.g. Gloeckler et al., 1986; Neugebauer et al. (2007), Chaizy et al. 1991, Gilbert et al., 2015, Burch et al. 2015, Gombosi et al. 2015]. Neugebauer et al. [2007] describes an in-situ encounter of the Ulysses spacecraft with the ion tail of comet McNaught. Ulysses first detected the comet on February 4th, 2007 and it was noticeable in data from multiple instruments onboard until just before the 8th of February. During this period, the comet had measurable effects on the kinetic properties of the solar wind, including ion heating and the production of compressional waves in the magnetic field, all of which are evidence of mass loading during the pickup process. During this period, a number of singly ionized pick up ions were observed with SWICS indicating the presence of pickup ions of C^+ , N^+ , O^+ , OH^+ , H_2O^+ , H_3O^+ , Ne^+ and other molecules as well as other low charge ions not of solar origin. Burch et al. (2015) and Gombosi et al. (2015) discuss the detection of negatively charge molecular clusters, most likely water clusters with large masses, near Rosetta. These were found at a distance of 100 km from the comet nucleus and likely persist for on the order of a day (Gombosi et al. 2015).

Measurement Objective 2: Negative ions from the Moon

The Moon's tenuous atmosphere is formed by a variety of mechanisms including interior release, particle sputtering, photon-stimulated desorption, chemical sputtering, thermal desorption, and meteoritic impacts (Stern et al. 1999). The most abundant species are He, Na, K and Ar at densities up to 10^4 cm^{-3} (Hoffman et al., 1973; Hartle and Thomas, 1974; Sarantos et al., 2012b). Curiously, the composition of the lunar atmosphere is still not well known (Wurz et al., 2007; Stern et al., 1999). This collisionless atmosphere (exosphere) can easily be lost by gravitational escape, chemical loss and condensation, ionization and pickup by the solar wind (Stern, 1999). Ionization and pickup are particularly important processes for ions heavier than Helium. The first observation of lunar ions was of Si/Al⁺ and O⁺ by the AMPTE spacecraft (Hilchenbach et al., 1993). Shortly thereafter, Mall et al. [1998] reported these ions as well as possibly P⁺ using measurements from the Wind Spacecraft. More recently, He⁺, C⁺, O⁺, Na⁺ and K⁺ were detected by the SELENE (Kaguya) spacecraft (Yokota et al., 2009). Hartle and Killen (2006) showed that these ions could be used to detect lower density exospheric species, owing to the very high sensitivity of ion composition spectrometers when compared with neutral mass spectrometers. Using well-known models of lunar exospheric neutral atoms (Hartle and Thomas, 1974; Sarantos et al., 2012a), Sarantos et al. (2012b) showed that fluxes of 15×10^4 and $6 \times 10^4 \text{ cm}^{-2} \text{ s}^{-1}$ for He⁺ and Na⁺ could be regularly expected.

Despite the fact that measurements of ions at the moon have so far all been positive, negative ions are also expected. Ion sputtering and electron stimulated desorption (ESD) result in both positive and negative ions, with the resulting charge depending on a number of factors including: surface composition and conductivity, the incident sputtering ion, and incident ion energy [Deng et al., 2001; Chiba, 2010, Wurz et al., 2007]. Lanzillotto et al. [1991] showed from laboratory experiments that O⁻ and Si⁻ are produced, along with their positive counterparts, by ESD from SiO₂ surfaces.

Negative ions are expected to make up a small fraction (1-10%) of the ionized material in the lunar exosphere, formed mainly by the interaction of solar wind protons with the lunar regolith ("topsoil") or by micrometeorite impacts on the surface [Wekhof 1981, 1980]. A larger fraction is expected near shaded regions or on the night-side of the moon, where the surface becomes negatively charged and expels negatively charge dust and plasma [Farrell et al. 2007]. The Lunar regolith is composed of roughly 60% oxygen, 17% silicon, 7% aluminum and a few percent of many other species, mostly metals [Vorburger et al., 2014]. Secondary ion production by sputtering is strongly enhanced by the high oxygen abundance in lunar regolith [Maul and Wittmack, 1975]. The combination of these factors is expected to result in O⁻ dominating the ionized component of oxygen [Lanzillotto et al., 1991; Chiba, 2010] and possibly the ionized component as a whole. As such, observing O⁻ is key to understanding the ionized lunar exosphere and its coupling to the lunar surface via space weathering processes. There are no successful observations of these negative ions near the Moon. The lunar flyby segment of the proposed mission should provide a prime opportunity to study unobserved portions of the Moon's atmosphere through its negative ion composition. Measurements of planetary pickup ions were successfully made using AIPS heritage technologies and demonstrate that negatively charged ions would be well resolved with AIPS [Zurbuchen et al., 2011; Raines et al., 2013].

3. An Anion Focused Investigation

The AIPS sensor is based on the Fast Imaging Plasma Spectrometer (FIPS) on NASA's MErcury Surface, Space ENvironment, Geochemistry and Ranging (MESSENGER) mission [Solomon *et al.*, 2007], which successfully measured the plasma environment of Mercury from 2011-2015 and has been used to map multiple ion species (H^+ through Ca^+). FIPS was a time of flight plasma mass spectrometer to orbit Mercury from 2011 to 2015. It measured ions from the solar wind as well as from Mercury's space environment. FIPS instrument characteristics are shown in Table 1. In addition to making the first solar wind measurements at 0.3 AU in the last 30 years [Gershman *et al.*, 2012], FIPS made the first observations of He⁺ pickup ion distributions at radial distances of 0.3 – 0.7 AU from the Sun [Gershman *et al.*, 2013]. In this work, the gravitational focusing cone was examined and comparisons were made with ACE/SWICS [Gloeckler *et al.*, 1997] measurements at 1 AU. In a follow-on work, Gershman *et al.* [2014] examined partial 3D velocity distribution functions for pickup He⁺. That study found that this distribution decreases nearly monotonically with increasing pitch angle, in contrast to the typical isotropic or spherical distributions more commonly assumed. FIPS also made the first ever observations of ions from Mercury itself, including He⁺, O⁺ and Na⁺, and found that they are concentrated at the magnetospheric cusps and central plasma sheet [Zurbuchen *et al.*, 2008; 2011]. These ions were observed throughout Mercury's space environment, with an average observed density of $5.1 \times 10^{-3} \text{ cm}^{-3}$ for Na⁺-group ions (Na⁺, Mg⁺ and Si⁺) [Raines *et al.*, 2013]. Within the magnetosphere, FIPS observed precipitation of solar wind protons in the northern cusp, as well as population of Na⁺-group ions that appeared to be upwelling there [Raines *et al.*, 2014]. This data also showed that Na⁺-group ions can be dynamically important in Mercury's plasma sheet, reaching up to 50% of mass density in that region [Gershman *et al.*, 2014].

The AIPS instrument draws strongly from FIPS heritage and was designed to fit within a 6U CubeSat bus as well as be adapted for negative ions. These negative ion measurements will be carried out using the same principles of operation as FIPS, but with voltages optimized to accommodate negative ions as shown in Figure 3. 3U will be reserved for the electrostatic analyzer, time-of-flight telescope, and the main electronics assemblies that control the science instrument as shown in Figure 2. The AIPS instrument is expected to weigh <2kg, supported by its flight heritage [Andrews *et al.*, 2007], and can be well within the required 14 kg mass limit for the entire CubeSat.

Table 1. FIPS characteristics (from Andrews *et al.*, 2007)

<u>Characteristic</u>	<u>Value</u>
Mass	1.41 kg

Volume	17.0 x 20.5 x 18.8 cm ³
Power average/maximum	1.9 / 2.1 W
Scan Speed	64s / 10s
FOV	1.4 π sr
Energy range	<0.010 – 20 keV/e
M/q range	1-60 amu/e at solar wind velocities
Average efficiency	0.2
Geometric Factor	1 x 10 ⁻³ cm ² sr eV/eV

3.1 Mission Concept

AIPS is a targeted, low-resource instrument designed to measure negative particles originating from planetary bodies and within the heliosphere. We now outline the AIPS instrument concept, beginning with a discussion of the principle of operation of an instrument suitable for operation on a small satellite.

3.1.1 Particle Measurements with AIPS

AIPS can measure negative ions with energy per charge (E/q) of 0.05 – 20 keV/e, with an energy resolution of about 6%. This energy range overlaps the energy range of CASSINI/ELS, and that of Rosetta/IES, which both successfully measured negative particles in-situ. It can measure ions with mass per charge ratios (m/q) of 1 – 60 amu/e at solar wind velocities (\geq 400km/s) and a much larger mass per charge range at much lower velocities. The maximum m/q allowed by the sensor depends on the velocity of the particle and on the length of the time of flight window. Using a flexible field programmable gate array (FPGA, e.g. Rogacki and Zurbuchen 2013) as a timing solution, with a timing resolution on the order of a \sim 2 ns, and an adjustable window up to several 10s of microseconds, AIPS would be able to retrieve measurements of masses up to 10⁵ amu/e.

Previous measurements of pickup ions and charged nanograins (\sim 10²- 10⁵ amu/e) with velocities in the range of hundreds of m/s have shown that their energy is broadly distributed over this energy range (e.g., Burch et al. 2015, Hill et al. 2012, Teolis et al 2010). AIPS records the incident angle of all measured particles as they enter its wide (1.4 π sr) instantaneous field-of-view (FOV), with an angular resolution of about 15°. These measurements allow separation of negative particles by m/q as well as characterization of their velocity distribution functions. Singly ionized species can be separated by mass, as their charge is unity.

The optical subassemblies of the AIPS instrument include an electrostatic analyzer (ESA) and a time-of-flight (TOF) telescope joined by a post-acceleration transition region as shown in the top half of Figure 3. The instrument electronics are comprised of an instrument control board with a field programmable gate array (FPGA) central to instrument operations, as well as three power supplies to provide swept electrode potentials in the ESA and steady-state biases in the TOF telescope. The AIPS instrument block diagram is shown in the bottom half of Figure 3.

3.1.2 Instrument Overview

The hourglass-shaped ESA, shown in the upper left quadrant of Figure 3, uses a voltage applied to curved electrodes to select particles on the basis of their E/q . Negative ions must fall within ~6% of the target E/q in order to pass through the ESA without hitting the walls. The ESA voltage may be logarithmically stepped over 60 steps, admitting negative ions from -0.05 keV/e to -20 keV/e over the full energy scan. Besides E/q filtering, the complex geometry of the ESA serves to keep out UV light that would be a source of background in the detectors [Gilbert et al., 2014]. The post-acceleration region is the transition between the ESA collimators and the TOF telescope, which is maintained at a positive potential of 10 kV. As negative ions exit the ESA, they gain kinetic energy in proportion to their integer charge state as they pass through this potential, thus allowing improved mass separation. Negative ions then impact a thin layer of elemental carbon, known as a carbon foil. Here the negative ions experience some mass-dependent angular scattering and energy loss (1-5 keV) while passing through, which is partially mitigated by the energy gained in the post-acceleration region. As they pass through the carbon foil, the negative ions eject secondary electrons (~1-10 electrons depending on the incident energy) from the surface of the foil and emerge into TOF telescope. These secondary electrons are deflected by an electrostatic mirror harp onto a position-sensitive micro-channel plate (MCP) detector assembly, where they will trigger a TOF start signal. While the majority of negative ions will exit the carbon foil as neutrals, the charge state of the emerging particle does not change the measurement principle in the TOF telescope. The particle continues on a straight trajectory to hit the stop MCP detector assembly, triggering a TOF stop signal. The impact location of a particle on the MCP is governed by the incident angle of the original anion into the AIPS aperture. This mapping is most easily understood in a polar coordinate system on the MCP where the radius is related to the zenith angle of the anion in FOV and the azimuthal angle on the MCP is the same as the azimuthal angle of the anion in FOV. The net result is the measurement of incident angles, E/q and TOF for individual negative ions. Any ambient electrons from the local space environment that pass through the ESA into the TOF chamber can be suppressed based on their low mass per charge and TOF (<2ns) compared to that of negatively charge nanograins and anions [Funsten et al. 2013]. It is also worth noting that the flux of ambient electrons over the AIPS energy range is expected to be very low, as the energy distribution falls off significantly beyond $E > 1$ keV to $\ll 10^{-6}$ of the total electron density (Yoon et al. 2016 and references therein).

3.1.3 Measurement Concept

The AIPS sensor measures E/q , TOF, and incident angle, with one complete scan over the full range of E/q values every 8 s. AIPS has a very large instantaneous and conical FOV of approximately 1.4π sr, extending within polar angles $15^\circ - 75^\circ$ (from the sensor symmetry axis), and a full 360° in azimuth. The sensor has an approximate angular resolution of 15° throughout the entire FOV. The incident direction of any particle is derived through a two-dimensional imaging process, as described previously. The large FOV can be increased through slow spinning of the spacecraft, giving an effective FOV of $\sim 3\pi$ sr. This can maximize chances of detection of negative ions in all mission phases, which is particularly important in this exploratory mission.

While we have largely focused on the detection of individual ions with predecessors like FIPS, AIPs can also detect molecules, for example negatively charge water clusters. As long as the E/q of negatively charge clusters falls within the measurement range, particles will pass through the ESA and impact the carbon foil. They may or may not break into their constituents in the carbon foil, but regardless, their velocity and total energy will be measured in the TOF telescope. Continued statistical sampling should reveal the composition of the dust clusters and the associated daughter products, using the principles described in Young et al. (2004).

AIPS can produce two main types of data: 1) Count rate spectra, made from counts summed over all angles but separated by E/q . These have are used both to verify the proper operation of AIPS and for improved statistics in scientific studies. 2) Anion event data, each containing the measured TOF, MCP position, and E/q value for an individual ion that was measured by AIPS. Ion events are the primary data product, used for the highest resolution studies of negative ion composition and kinetic properties. The instrument can be operated continuously through all mission phases, and data can be stored onboard between downlink passes.

Using previous results, we can estimate the incident flux expected in several different environments. *Elphic et al.* [1991] used laboratory measurements of secondary ions from lunar soil simulants to predict secondary ion flux from typical solar wind sputtering. They reported fluxes of $2-6 \times 10^3 \text{ cm}^{-2} \text{ s}^{-1}$ for Si^+ , Na^+ , Mg^+ and Al^+ , at the surface. Given the exceptional nature of O^- production described above, its flux should be at least as large. To estimate counts that would be measured by AIPS, we went through several steps. Starting with a surface flux of $2 \times 10^3 (\text{cm}^2 \text{ s})^{-1}$, we computed the lunar pick-up ion flux at 50 km (Φ_{ipa}) altitude using a $1/R^2$ reduction, where the lunar radius (R) is 1741 km. We then computed the total counts from the following well-known equation,

$$N = \eta g \int_{v_1}^{v_2} f(v) v^3 dv$$

where we used the average efficiency (η) and geometric factor (g) listed in Table 1. We assumed a simple isotropic distribution function ($f(v)$) for the picked up O^- ions, which is constant from

rest through twice the solar wind speeds ($2 v_{sw}$) [Gloeckler *et al.*, 1997]. Using the first moment of the distribution function integrated over all space yields the following simple result:

$$f(v) = \frac{\Phi_{lpa}}{4v_{sw}^4}$$

When integrated over velocities corresponding to AIPS energy range, AIPS would measure O^- count rates of $3.6 \times 10^{-2} s^{-1}$ or about $130 h^{-1}$. While this count rate is very low, double-coincidence detection method, utilized by AIPS, has very low background rates, thus making detection of these rare negative ions possible.

We can estimate the counts due to negatively charged nanograins during cometary trail encounters by comparison with Rosetta measurements near 3 AU [Gombosi *et al.* 2015; Burch *et al.*, 2015). After integrating a linear approximation of their measured flux of $10^4 - 10^6 (cm^2 s eV sr)^{-1}$ in the 0.1 – 1 keV range (their Figure 5 left), we estimated that AIPS would measure total counts of about $9 \times 10^4 s^{-1}$. The same can be done for water clusters measured by Cassini/ELS at Enceladus [Hill *et al.*, 2012]. From their Figure 4, we approximate ELS counts in the 1000 – 10000 eV range to follow a linear trend ranging from $10^3 - 10^6$ counts/s. After converting these count rates to flux using the published geometric factor for ELS [Young *et al.*, 2004], we integrated over the AIPS energy range to estimate AIPS counts at $1.3 \times 10^9 s^{-1}$. These count rates are summarized in Table 2.

Estimating the flux of O^- ions from heliospheric dust is much more difficult, due in part to the fact that there is little consensus about densities, radial distributions and sizes of the dust grains [Mann *et al.*, 2004]. Furthermore, estimated short lifetimes of singly, negatively charged ions (on the order of second) due photo-detachment from solar UV (Wekhof *et al.* 1981), make detection more difficult. We were able to roughly estimate the flux at 1 AU of these heliospheric pick-up anions (Φ_{hpa}) using the equation below:

$$\Phi_{hpa} = \Phi_{sputter} \sigma_{dust} (\Phi_{dust} / v_{dust}) (v_{sw} \tau)$$

We used $2 \times 10^3 (cm^2 s)^{-1}$ for the sputtering flux ($\Phi_{sputter}$) [Elphic *et al.*, 1991], $7.9 \times 10^{-13} cm^2$ as the average dust particle area, and $0.1 (cm^2 s)^{-1}$ for the estimated dust flux (Φ_{dust}) [Shippers *et al.*, 2015], an anion lifetime (τ) of 1 s [Wekhof *et al.*, 1981], 20 km/s for the estimated dust speed (v_{dust}) and a solar wind speed of 400 km/s. The resulting flux of $3.2 \times 10^{-9} (cm^2 s)^{-1}$ and estimated count rate of $2.2 \times 10^{-10} s^{-1}$ makes clear the idea that quantitatively measuring anions from heliospheric dust would take a much larger instrument and long integration times..

Table 2. Expected flux and AIPS count rates for sources described in text. We used the published value of ELS geometric factor, $1.4 \times 10^{-2} cm^2 sr eV/eV$, to convert counts to flux in item 3.

Source	Expected Flux	Expected Counts
Lunar anions (@ 50 km alt.)	$1.9 \times 10^3 (cm^2 s)^{-1}$	$3.6 \times 10^{-2} s^{-1}$
Cometary nano-grains (@ 100 km alt.)	$10^4 - 10^6 (cm^2 s eV sr)^{-1}$	$9 \times 10^4 s^{-1}$
Enceladus water clusters (@ ~25 km alt.)	$7 \times 10^4 - 7 \times 10^7 (cm^2 s eV)^{-1}$	$7 \times 10^7 s^{-1}$
Heliospheric pick-up anions (@ 1 AU)	$3.2 \times 10^{-9} (cm^2 s)^{-1}$	$2.2 \times 10^{-10} s^{-1}$

4. Conclusions

Measurements of negative particles at satellites of gas giants, near comets, in the vicinity of the Moon, or elsewhere in the heliosphere offer insight into the extended and localized sources of pickup ions in the solar system and also the interaction processes that shape these sources. We described an instrument concept, AIPS, that targets such observations for the first time, with a dedicated anion mass spectrometer, and describe how these new measurements can contribute to our knowledge of this underexplored population. We also showed that this instrument could be built small enough to fit on a notional 6U CubeSat missions, coined here as SAILS.

If successful as part of a targeted mission, AIPS can provide the first systematic survey of negative nanograins and anions and near moons and in the heliosphere, particularly near comets, closely examining the spatial variation and time dependences in an effort to identify sources and conditions that produce negative particles. Understanding the nature of negative particles in the heliosphere will advance our knowledge of how mass is partitioned between anion, ion, and neutral populations and create a more complete picture of our solar system and local place in the Galaxy.

Acknowledgments and Data

The authors would like to acknowledge helpful conversations with G. Gloeckler, T. Gombosi, and R. Lundgren and other members of the Solar and Heliospheric Research Group at the University of Michigan. The authors would like to thank the University of Michigan for its financial and administrative support. No datasets were analyzed for this publication.

Author Manuscript

References

- Adriani, O., et al. (2011), The Discovery of Geomagnetically Trapped Cosmic-ray Antiprotons, *The Astrophysical Journal*, 737, L29- doi: 10.1088/2041-8205/737/2/L29.
- Andrews, G. B., T. H. Zurbuchen, B. H. Mauk, H. Malcom, L. A. Fisk, G. Gloeckler, G. C. Ho, J. S. Kelley, P. L. Koehn, T. W. Lefevre, S. S. Livi, R. A. Lundgren, and J. M. Raines (2007), The Energetic Particle and Plasma Spectrometer Instrument on the MESSENGER spacecraft, *Space Sci. Rev.*, 131, 523–556, doi:10.1007/s11214-007-9272.
- Borucki, W. J., R. C. Whitten, E. L. O. Bakes, E. Barth, and S. Tripathi (2006), Predictions of the electrical conductivity and charging of the aerosols in Titan's atmosphere, *Icarus*, 181, 527-544, doi: 10.1016/j.icarus.2005.10.030.
- Burch, J. L., T. I. Gombosi, G. Clark, P. Mokashi, and R. Goldstein (2015a), Observation of charged nanograins at comet 67P/Churyumov-Gerasimenko, *Geophys. Res. Lett.*, 42, 6575–6581, doi:10.1002/2015GL065177.
- Burch, J. L., T. E. Cravens, K. Llera, R. Goldstein, P. Mokashi, C.-Y. Tzou, and T. Broiles (2015b), Charge exchange in cometary coma: Discovery of H ions in the solar wind close to comet 67P/Churyumov-Gerasimenko, *Geophys. Res. Lett.*, 42, 5125–5131, doi:10.1002/2015GL064504.
- Chaizy, P., H. Reme, J. A. Sauvaud, C. D'Uston, R. P. Lin, D. E. Larson, D. L. Mitchell, K. A. Anderson, C. W. Carlson, A. Korth, and D. A. Mendis (1991), Negative ions in the coma of Comet Halley, *Nature*, 349, 393-396, doi: 10.1038/349393a0.
- Chiba, K. (2010), Analysis of intensities of positive and negative ion species from silicon dioxide films using time-of-flight secondary ion mass spectrometry and electronegativity of fragments, *Applied Surface Science*, 256, 1641-1646, doi: 10.1016/j.apsusc.2009.09.085.
- Coates, A. J., F. J. Crary, G. R. Lewis, D. T. Young, J. H. Waite, and E. C. Sittler (2007), Discovery of heavy negative ions in Titan's ionosphere, *Geophysical Research Letters*, 34, 22103- doi: 10.1029/2007GL030978.
- Coates, A. J., G. H. Jones, G. Lewis, A. Wellbrock, D. T. Young, F. J. Crary, R. E. Johnson, and T. W. Hill (2009), Negative Ions in the Enceladus Plume (Invited), AGU Fall Meeting Abstracts.

- Coates, A.J., A. Wellbrock, G.R. Lewis, G.H. Jones, D.T. Young, F.J. Crary, J.H. Waite Jr., Heavy negative ions in Titan's ionosphere: altitude and latitude dependence, *Planet. Space Sci.*, 57, Issues 14-15, 1866-1871, doi:10.1016/j.pss.2009.05.009, (online May, print Dec) 2009.
- Coates, A.J., A. Wellbrock, G.R. Lewis, G.H. Jones, D.T. Young, F.J. Crary, J.H. Waite, R.E. Johnson, T.W. Hill, E.C. Sittler Jr., Negative ions at Titan and Enceladus: recent results, *Faraday Disc.*, 147(1), 293-305, DOI: 10.1039/C004700G2010, Nov 2010.
- Coates, A.J., G.H. Jones, G.R. Lewis, A. Wellbrock, D.T. Young, F.J. Crary, R.E. Johnson, T.A. Cassidy, T.W. Hill, Negative Ions in the Enceladus Plume, *Icarus*, 206, 618-622, doi:10.1016/j.icarus.2009.07.013, Apr 2010.
- Coates, A.J., Ion Pickup and Acceleration: Measurements From Planetary Missions, in 'Physics of the heliosphere: a 10-year retrospective', 10th Annual Astrophysics Conference, AIP proceedings volume 1436, ISBN: 978-0-7354-1026-8, Editor(s): Jacob Heerikhuisen, Gang Li, Nikolai Pogorelov, Gary Zank, p89-102, May 2012.
- Coates, A.J., J.L. Burch, R. Goldstein, H. Nilsson, G. Stenberg Wieser, E. Behar and the RPC team, Ion pickup observed at comet 67P with the Rosetta Plasma Consortium (RPC) particle sensors: similarities with previous observations and AMPTE releases, and effects of increasing activity, *J. Phys.: Conf. Ser.* 642 012005, Oct 2015.
- Coates, A.J., Johnstone, A.D., Huddleston, D.E., Wilken, B., Jockers, K. and Glassmeier, K.-H., 1988, 'Velocity space diffusion of pick-up ions from the water group at Comet Halley', *J. Geophys. Res.*, 94, p9983-9993, 1989; correction 95, p4343, 1990.
- Coates, A.J., Johnstone, A.D., Wilken, B. and Neubauer, F.M., 'Velocity space diffusion and non-gyrotropy of pickup water group ions at comet Grigg-Skjellerup', *J. Geophys. Res.*, 98, 20,985-20,994, 1993.
- Coates, A.J., Wilken, B., Johnstone, A.D., Jockers, K., Glassmeier, K.-H. and Huddleston, D.E., 'Bulk properties and velocity distributions of water group ions at comet Halley: Giotto measurements', *J. Geophys. Res.*, 95, 10249-10260, 1990.
- Cutler, J., Ridley, A. and A. Nicholas. "Cubesat Investigating Atmospheric Density Response to Extreme Driving (CADRE)." In proceedings of the 25th Annual AIAA/USU Conference on Small Satellites. SSC11-IV-7. August 2011.
- Deng, Z. W. and R. Souda (2001), A SIMS study on positive and negative ions sputtered from graphite by mass-separated low energy Ne^+ , N_2^+ and N^+ ions, *Nuclear Instruments and Methods in Physics Research B*, 183, 260-270, doi: 10.1016/S0168-583X(01)00742-X.

- Domingue, D. L., C. R. Chapman, R. M. Killen, T. H. Zurbuchen, J. A. Gilbert, M. Sarantos, M. Benna, J. A. Slavin, D. Schriver, P. M. Tr´víccaron;ek, T. M. Orlando, A. L. Sprague, D. T. Blewett, J. J. Gillis-Davis, W. C. Feldman, D. J. Lawrence, G. C. Ho, D. S. Ebel, L. R. Nittler, F. Vilas, C. M. Pieters, S. C. Solomon, C. L. Johnson, R. M. Winslow, J. Helbert, P. N. Peplowski, S. Z. Weider, N. Mouawad, N. R. Izenberg, and W. E. McClintock (2014), Mercury's Weather-Beaten Surface: Understanding Mercury in the Context of Lunar and Asteroidal Space Weathering Studies, *Space Science Reviews*, 181, 121-214, doi: 10.1007/s11214-014-0039-5.
- Elphic, R. C., H. O. Funsten, B. L. Barraclough, D. J. McComas, M. T. Paffett, D. T. Vaniman, and G. Heiken(1991), Lunar surface composition and solar wind-induced secondary ion mass spectrometry, *Geophys. Res. Lett.*, 18, 2165–2168, doi:10.1029/91GL02669.
- Farrell, W. M., Stubbs, T. J., Vondrak, R. R., Delory, G. T. and J. S. Halekas (2007), Complex electric fields near the lunar terminator: The near-surface wake and accelerated dust, *Geophysical Research Letters*, 34, doi:10.1029/2007GL029312
- Frisch, P. C., J. M. Dorschner, J. Geiss, J. M. Greenberg, E. Grun, M. Landgraf, P. Hoppe, A. P. Jones, W. Kratschmer, T. J. Linde, G. E. Morfill, W. Reach, J. D. Slavin, J. Svestka, A. N. Witt, and G. P. Zank (1999), Dust in the Local Interstellar Wind, *The Astrophysical Journal*, 525, 492-516, doi: 10.1086/307869.
- Funsten, H. O., et al. (2013), Reflection of solar wind hydrogen from the lunar surface, *J. Geophys. Res. Planets*, 118, 292–305, doi:10.1002/jgre.20055.
- Funsten, H.O., D.J. McComas, and B.L. Barraclough, "Application of Thin Foils in Low-energy Neutral-atom Detection", *Proc. SPIE*, 1744, 62-69, 1992
- Geiss, J., Gloeckler, G., & von Steiger, R. (1995), Origin of the solar wind from composition data, *Space Sci. Rev.*, 72, 49.
- Gershman, D. J., J. A. Slavin, J. M. Raines, T. H. Zurbuchen, B. J. Anderson, H. Korth, D. N. Baker, and S. C. Solomon (2013), Magnetic flux pile-up and plasma depletion in Mercury's subsolar magnetosheath, *J. Geophys. Res. Space Physics*, 118, 7181–7199, doi:10.1002/2013JA019244.
- Gershman, D. J., J. A. Slavin, J. M. Raines, T. H. Zurbuchen, B. J. Anderson, H. Korth, D. N. Baker, and S. C. Solomon (2014), Ion kinetic properties in Mercury's pre-midnight plasma sheet, *Geophys. Res. Lett.*, 41,5740–5747, doi:10.1002/2014GL060468.
- Gershman, D. J., T. H. Zurbuchen, L. A. Fisk, J. A. Gilbert, J. M. Raines, B. J. Anderson, C. W. Smith, H. Korth, and S. C. Solomon (2012), Solar wind alpha particles and heavy ions in the inner heliosphere observed with MESSENGER, *J. Geophys. Res.*, 117, A00M02, doi:10.1029/2012JA017829.
- Gilbert et al. (2014) Characterization of Background Sources in Space-Based Time-of-Flight Mass Spectrometers, *Rev. Sci. Instrum.*, 85, 091301.

- Gilbert, J. A., et al. (2015), In Situ Plasma Measurements of Fragmented Comet 73P Schwassmann-Wachmann 3, *Astrophys. J.*, 815, 1-12, doi:10.1088/0004-637X/815/1/12.
- Gloeckler G 1986 Cometary pick-up ions observed near Giacobini-Zinner *Geophys. Res. Lett.* 13 251
- Gloeckler, G. and J. Geiss (1998), Interstellar and Inner Source Pickup Ions Observed with SWICS on ULYSSES, *Space Science Reviews*, 86, 127-159, doi: 10.1023/A:1005019628054.
- Gloeckler, G., L. A. Fisk, and J. Geiss (1997), Anomalously small magnetic field in the local interstellar cloud, *Nature*, 386, 374-377, doi: 10.1038/386374a0.
- Gloeckler, G., L. A. Fisk, J. Geiss, N. A. Schwadron, and T. H. Zurbuchen (2000), Elemental composition of the inner source pickup ions, *Journal of Geophysical Research*, 105, 7459-7464, doi: 10.1029/1999JA000224.
- Gloeckler, G., Schwadron, N. A., Fisk, L. A., and Geiss, J.: (1995), Weak pitch angle scattering of few MV rigidity ions from measurements of anisotropies in the distribution function of interstellar pickup H^+ , *Geophys. Res. Lett.* 22, p2665.
- Gombosi, T. I., Burch, J. L. and M. Horányi (2015), Negatively charged nano-grains at 67P/Churyumov-Gerasimenko, *A&A*, 58, A23, DOI: <http://dx.doi.org/10.1051/0004-6361/201526316>
- Halekas, J. S., et al. (2015), MAVEN observations of solar wind hydrogen deposition in the atmosphere of Mars, *Geophys. Res. Lett.*, 42, 8901–8909, doi:10.1002/2015GL064693.
- Hargreaves, J. K. (1992), *The Solar-Terrestrial Environment*, Cambridge Atmos. Space Sci. Ser., vol. 5, Cambridge Univ. Press, Cambridge, U. K.
- Hartle, R. E. and G. E. Thomas (1974), Neutral and ion exosphere models for lunar hydrogen and helium, *Journal of Geophysical Research*, 79, 1519- doi: 10.1029/JA079i010p01519.
- Hartle, R. E. and R. Killen (2006), Measuring pickup ions to characterize the surfaces and exospheres of planetary bodies: Applications to the Moon, *Geophysical Research Letters*, 33, 5201- doi: 10.1029/2005GL024520.
- Hilchenbach, M., D. Hovestadt, B. Klecker, and E. Moebius (1993), Observation of energetic lunar pick-up ions near earth, *Adv. Space Res.*, 13, 321-324, doi: 10.1016/0273-1177(93)90086-Q.
- Hill, T. W., M. F. Thomsen, R. L. Tokar, A. J. Coates, G. R. Lewis, D. T. Young, F. J. Crary, R. A. Baragiola, R. E. Johnson, Y. Dong, R. J. Wilson, G. H. Jones, J.-E. Wahlund, D. G. Mitchell, and M. Horanyi (2012), Charged nanograins in the Enceladus plume, *Journal of Geophysical Research (Space Physics)*, 117, 5209- doi: 10.1029/2011JA017218.

- Hoffman, J. H., R. R. Hodges Jr., F. S. Johnson, and D. E. Evans (1973), Lunar atmospheric composition results from Apollo 17, Lunar and Planetary Science Conference Proceedings, 4, 2865.
- Jackson W M (1992), Formation of ions and radicals from icy grains in comets Asteroids, Comets, Meteors 1991 (Houston, TX: Lunar and Planetary Institute) pp 249–52.
- Jones, G.H., C. S. Arridge, A. J. Coates, G. R. Lewis, S. Kanani, A. Wellbrock, D. T. Young, F. J. Crary, R. L. Tokar, R. J. Wilson, T. W. Hill, R. E. Johnson, D. G. Mitchell, J. Schmidt, S. Kempf, U. Beckmann, C. T. Russell, Y. D. Jia, M. K. Dougherty, J. H. Waite Jr., B. Magee, Fine jet structure of electrically-charged grains in Enceladus' plume, *Geophys Res Letters*, vol 36, L16204, doi:10.1029/2009GL038284, Sep 2009
- Kallenbach, R., J. Geiss, G. Gloeckler, and R. von Steiger (2000), Pick-up Ion Measurements in the Heliosphere - A Review, *Astrophysics and Space Science*, 274, 97-114, doi: 10.1023/A:1026587620772.
- Klahr, H. H. and D. N. C. Lin (2001), Dust Distribution in Gas Disks: A Model for the Ring around HR 4796A, *The Astrophysical Journal*, 554, 1095-1109, doi: 10.1086/321419.
- Krüger, H., Strub¹, P., Grün, E., and V. J. Sterken, (2015) Sixteen years of *ulysses* interstellar dust measurements in the solar system. I. Mass distribution and gas-to-dust mass ratio, *The Astrophysical Journal*, 812, 2, 139.
- Lanzillotto, A.-M., T. E. Madey, and R. A. Baragiola (1991), Negative-ion desorption from insulators by electron excitation of core levels, *Physical Review Letters*, 67, 232-235, doi: 10.1103/PhysRevLett.67.232.
- Larsson, M., W. D. Geppert, and G. Nyman (2012), Ion chemistry in space, *Reports on Progress in Physics*, 75, 066901- doi: 10.1088/0034-4885/75/6/066901.
- Mahaffy, P. R., et al. (2014), The Neutral Mass Spectrometer on the Lunar Atmosphere and Dust Environment Explorer Mission, *Space Science Reviews*, 11- doi: 10.1007/s11214-014-0043-9.
- Mann I., Meyer-Vernet N. and Czechowski A. (2014), Dust in the planetary system: Dust interactions in space plasmas of the solar system, *Physics Reports*, Volume 536, Issue 1, p. 1-39.
- Mann, I., H. Kimura, D. A. Biesecker, B. T. Tsurutani, E. Grün, R. B. McKibben, J.-C. Liou, R. M. MacQueen, T. Mukai, M. Guhathakurta, and P. Lamy (2004), Dust Near The Sun, *Space Science Reviews*, 110, 269-305, doi: 10.1023/B:SPAC.0000023440.82735.ba.
- Mann, I., Murad, E., & Czechowski, A. 2007, *Planet. Space Sci.*, 55, 1000

- Maul, J. L. and K. Wittmack, Secondary ion emission from silicon and silicon dioxide, *Surf. Sci.*, 47, 358, 1975.
- McComas, D.J., N.A. Schwadron, F.J. Crary, H.A. Elliott, D.T. Young, J.T. Gosling, M.F. Thomsen, E. Sittler, J.-J. Berthelier, K. Szego and A.J. Coates, The interstellar hydrogen shadow: observations of interstellar pickup ions beyond Jupiter, *J. Geophys. Res.*, 109(A2), CiteID A02104 DOI: 10.1029/2003JA010217, 2004.
- Neugebauer, M., A.J. Lazarus, H. Balsiger, S.A. Fuselier, F.M. Neubauer and H. Rosenbauer, The velocity distributions of cometary protons picked up by the solar wind, *J. Geophys. Res.*, 94, 5227-5239, 1989
- Neugebauer, M., G. Gloeckler, J. T. Gosling, A. Rees, R. Skoug, B. E. Goldstein, T. P. Armstrong, M. R. Combi, T. Mäkinen, D. J. McComas, R. von Steiger, T. H. Zurbuchen, E. J. Smith, J. Geiss, and L. J. Lanzerotti (2007), Encounter of the Ulysses Spacecraft with the Ion Tail of Comet McNaught, *The Astrophysical Journal*, 667, 1262-1266, doi: 10.1086/521019.
- Olson, J., W. J. Miloch, S. Ratynskaia, and V. Yaroshenko, *Phys. Plasmas* 17(10), 102904 (2010). <https://doi-org.proxy.lib.umich.edu/10.1063/1.3486523>
- Raines, J. M., D. J. Gershman, J. A. Slavin, T. H. Zurbuchen, H. Korth, B. J. Anderson, G. Gloeckler, and S. C. Solomon (2014), Structure and dynamics of Mercury's magnetospheric cusp: MESSENGER measurements of protons and planetary ions, *J. Geophys. Res. Space Physics*, doi:10.1002/2014JA020120.
- Raines, J. M., D. J. Gershman, T. H. Zurbuchen, M. Sarantos, J. A. Slavin, J. A. Gilbert, H. Korth, B. J. Anderson, G. Gloeckler, S. M. Krimigis, D. N. Baker, R. L. McNutt, and S. C. Solomon (2013), Distribution and compositional variations of plasma ions in Mercury's space environment: The first three Mercury years of MESSENGER observations, *J. Geophys. Res.: Space Phys.*, 118, 1604–1619, doi:10.1029/2012JA018073.
- Rogacki, S., and T. H. Zurbuchen (2013), A time digitizer for space instrumentation using a field programmable gate array, *Rev. Sci. Instrum.* 84, 083107; doi: 10.1063/1.4818965
- Sarantos, M., R. E. Hartle, R. M. Killen, Y. Saito, J. A. Slavin, and A. Gloer (2012b), Flux estimates of ions from the lunar exosphere, *Geophysical Research Letters*, 39, 13101- doi: 10.1029/2012GL052001.
- Sarantos, M., R. M. Killen, D. A. Glenar, M. Benna, and T. J. Stubbs (2012a), Metallic species, oxygen and silicon in the lunar exosphere: Upper limits and prospects for LADEE measurements, *Journal of Geophysical Research (Space Physics)*, 117, 3103- doi: 10.1029/2011JA017044.

- Schippers *et al.*, (2015), Nanodust detection between 1 and 5 au using *Cassini* wave measurements, *ApJ*, 806, 77.
- Solomon, S. C., R. L. McNutt, R. E. Gold, and D. L. Domingue (2007), MESSENGER Mission Overview, *Space Sci. Rev.*, 131, 3–39, doi: 10.1007/s11214-007-9247-6.
- Stern, S. A. (1999), The lunar atmosphere: History, status, current problems, and context, *Reviews of Geophysics*, 37, 453-492, doi: 10.1029/1999RG900005.
- Teolis, B.D., G.H. Jones, P.F. Miles, R. L. Tokar, B. A. Magee, J. H. Waite, E. Roussos, D.T. Young, F. J. Crary, A. J. Coates, R. E. Johnson, W.-L. Tseng, R. A. Baragiola, 2010, Cassini finds an oxygen-carbon dioxide atmosphere at Saturn's icy moon Rhea, *Science*, 330 (6012), 1813-1815 doi: 10.1126/science.1198366
- Tokar, R.L., R.E.Johnson, M.F.Thomsen, E.C. Sittler, A.J. Coates, R.J. Wilson, F.J. Crary, D.T. Young, G.H. Jones, 2012, Detection of Exospheric O₂⁺ at Saturn's Moon Dione, *Geophys. Res. Lett.*, 39, L03105, 2012, doi:10.1029/2011GL050452.
- Vasyliunas, V. M. and G. L. Siscoe (1976), On the flux and the energy spectrum of interstellar ions in the solar system, *Journal of Geophysical Research*, 81, 1247-1252, doi: 10.1029/JA081i007p01247.
- Vorburger, A., P. Wurz, S. Barabash, M. Wieser, Y. Futaana, M. Holmstrom, A. Bhardwaj, and K. Asamura (2014), First direct observation of sputtered lunar oxygen, *Journal of Geophysical Research (Space Physics)*, 119, 709-722, doi: 10.1002/2013JA019207.
- Wekhof, A. (1981), Negative ions in the ionospheres of planetary bodies without atmospheres, *Moon and Planets*, 24, 45-52, doi: 10.1007/BF00897567.
- Wekhof, A.: (1980), *The Moon and Planets* 22, pp. 185–189.
- Wurz, P., U. Rohner, J. A. Whitby, C. Kolb, H. Lammer, P. Dobnikar, and J. A. Martin-Fernandez (2007), The lunar exosphere: The sputtering contribution, *Icarus*, 191, 486-496, doi: 10.1016/j.icarus.2007.04.034.
- Wurz, P., U. Rohner, J. A. Whitby, C. Kolb, H. Lammer, P. Dobnikar, and J. A. Martin-Fernandez (2007), The lunar exosphere: The sputtering contribution, *Icarus*, 191, 486-496, doi: 10.1016/j.icarus.2007.04.034.
- Yokota, S., et al. (2009), First direct detection of ions originating from the Moon by MAP-PACE IMA onboard SELENE (KAGUYA), *Geophys. Res. Lett.*, 36, L11201, doi:10.1029/2009GL038185.
- Young, D. T., et al. (2004), Cassini Plasma Spectrometer investigation, *Space Sci. Rev.*, 114, 1–4, doi:10.1007/s11214-004-1406-4.
- Yoon, Peter H. *et al* 2016 *ApJ* 826 204

- Zook, H. A. (1975), Hyperbolic cosmic dust - Its origin and its astrophysical significance, *Planetary and Space Science*, 23, 1391-1397, doi: 10.1016/0032-0633(75)90034-3.
- Zook, H. A. and O. E. Berg (1975), A source for hyperbolic cosmic dust particles, *Planetary and Space Science*, 23, 183-203, doi: 10.1016/0032-0633(75)90078-1.
- Zurbuchen, T. H., et al., (2008) MESSENGER observations of the composition of Mercury's ionized exosphere and plasma environment., *Science* 321, 90
doi:10.1126/science.1159314pmid:18599777
- Zurbuchen, T. H., J. M. Raines, J. A. Slavin, D. J. Gershman, J. A. Gilbert, G. Gloeckler, B. J. Anderson, D. N. Baker, H. Korth, S. M. Krimigis, M. Sarantos, D. Schriver, R. L. McNutt Jr., and S. C. Solomon (2011), MESSENGER observations of the spatial distribution of planetary ions near Mercury, *Science*, 333, 1862–1865,
doi:10.1126/science.1211302.

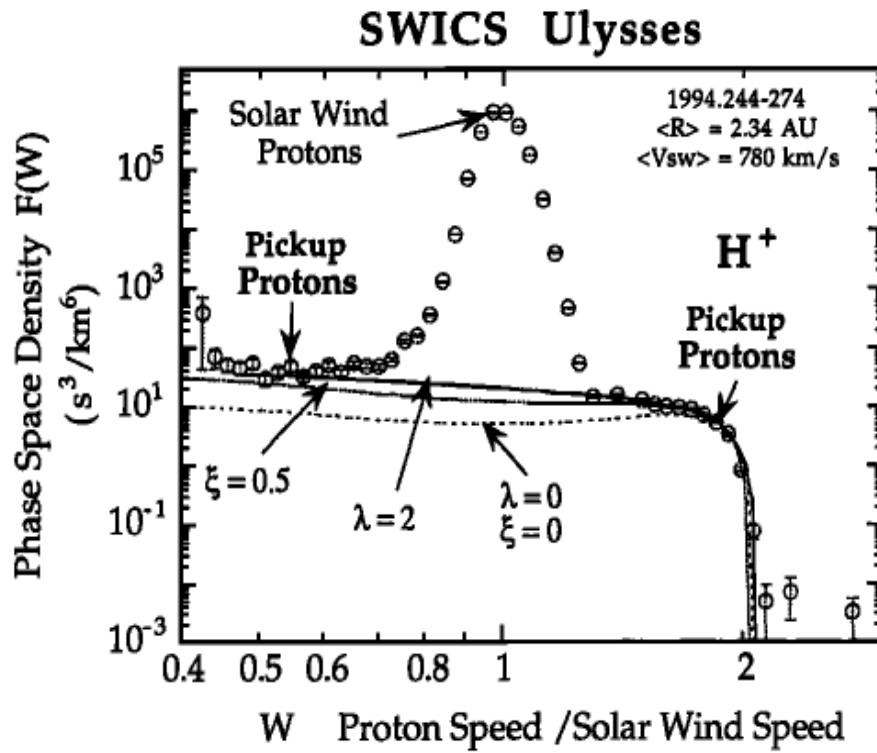
Figure Captions

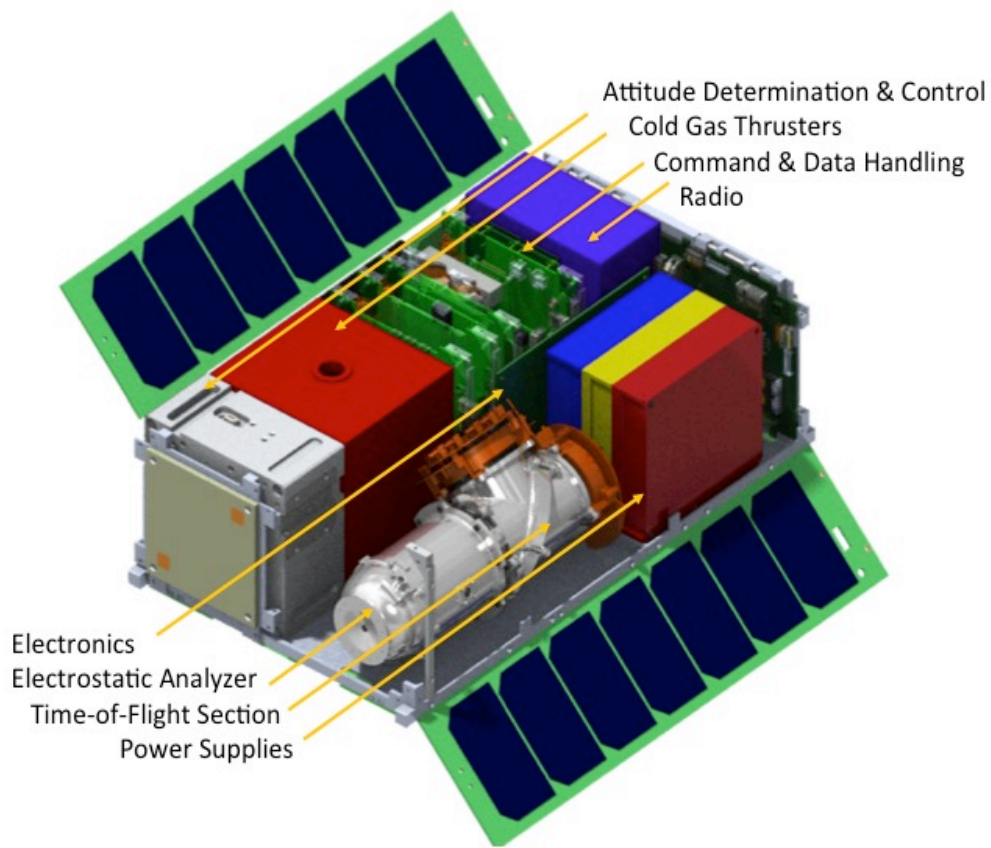
Figure 1. Pickup protons are superposed on the Gaussian solar wind proton velocity distribution. The pickup protons make up a flat distribution which rolls over at 2 solar wind speeds. (Adapted from Gloeckler et al., 1995).

Figure 2. CAD Model of the 6U Cubesat.

Figure 3. The cross section of AIPS is shown in the top half of the figure. Negative ions enter through the electrostatic analyzer on the left, pass through a post acceleration region where they gain $\sim 10\text{keV/e}$ of energy, and then pass through a carbon foil into the TOF telescope on the right hand side. The anion time of flight is measured by the pairing of start and stop MCPs. The bottom half of the figure shows the block diagram for AIPS and its interface to the sensor.

Author





Author N

